European Review for Medical and Pharmacological Sciences 2019; 23: 4164-4172

Circ-CCDC66 accelerates proliferation and invasion of gastric cancer *via* binding to miRNA-1238-3p

M. YANG, G.-Y. WANG, H. QIAN, X.-Y. JI, C.-Y. LIU, X.-H. ZENG, J. LV, Y.-X. SHI

Department of Gastroenterology, Hongkou Branch of Changhai Hospital, Navy Medical University (Second Military Medical University), Shanghai, China

Abstract. – OBJECTIVE: The aim of this study was to examine the expression of circ-CCDC66 in gastric cancer (GC) tissues and cell lines, as well as its correlation with the prognosis of GC. Moreover, the regulatory effects of circ-CCDC66 on biological behaviors of GC cells and its molecular mechanism were explored.

PATIENTS AND METHODS: The relative expression level of circ-CCDC66 in GC tissues and cell lines was determined by quantitative Real Time-Polymerase Chain Reaction (qRT-PCR). The correlation between the circ-CCDC66 level and overall survival of GC patients was analyzed as well. The potential influences of circ-CCDC66 on proliferative and invasive abilities of GC cells were evaluated through 5-Ethynyl-2'-deoxyuridine (EdU), colony formation and transwell assay, respectively. Meanwhile, the cell cycle progression and apoptosis of GC cells affected by circ-CCDC66 were determined. In addition, the direct target miRNA of circ-CCDC66 was predicted and verified by bioinformatics method and Dual-Luciferase reporter gene assay, respectively.

RESULTS: Circ-CCDC66 was significantly up-regulated in GC tissues and cell lines. Up-regulation of circ-CCDC66 indicated markedly worse prognosis of GC patients. Transfection of circ-CCDC66-siRNA remarkably attenuated proliferative and invasive abilities of BGC-823 and MGC-803 cells. Besides, GC cells were arrested in the G0/G1 phase, and the apoptotic rate was remarkably elevated after circ-CCDC66 knockdown. The Dual-Luciferase reporter gene assay verified that circ-CCDC66 bind to miRNA-1238-3p by competing with LHX2 (LIM-homeobox domain 2). MiRNA-1238-3p was significantly down-regulated in GC cells, whereas LHX2 was up-regulated. Furthermore, overexpression of miRNA-1238-3p in GC cells markedly suppressed the LHX2 level.

CONCLUSIONS: Circ-CCDC66 is highly expressed in GC tissues and cell lines. Knockdown of circ-CCDC66 attenuates proliferative and invasive abilities of GC cells. Our results indicate that circ-CCDC66/miRNA-1238-3p/LHX2 axis may be a promising target for GC treatment.

Key Words:
Gastric cancer (GC), Circ-CCDC66, Proliferation, Invasion.

Introduction

Gastric cancer (GC) is a common malignancy in the digestive system, with high morbidity and mortality. The incidence of GC remains high over the world, especially in Asia. The occurrence and development of GC are complex involving both internal and external factors. From the perspective of pathogenic biology, *Helicobacter pylori* infection is closely correlated with GC development[1]. Meanwhile, the pathogenesis of GC is related to dietary, lifestyle and genetic factors as well[2]. Clinical symptoms of early-stage GC are concealed. GC patients are prone to experience peritoneal, local and distant metastases at advanced stages. Currently, the 5-year survival of advanced GC is less than 20%. If precise diagnosis and comprehensive treatment are performed in time before tumor invasion of the basement membrane, the 5-year survival of GC patients may be up to 90%[3]. Hence, searching for molecular hallmarks of GC contributes to improving its diagnostic rate at an early stage.

CircRNAs are a kind of non-coding RNAs with diverse functions. It has been found that circRNA is widely distributed in the cytoplasm of eukaryotic cells, and is mainly produced by variable shear processing of precursor mRNA (pre-mRNA)[4]. Recent studies have identified important regulatory functions of circRNAs. In particular, circRNA can competitively bind to intracellular miRNAs as a miRNA sponge, thereby blocking the effect of miRNAs on target genes. Meanwhile, it regulates parental gene expressions, as well as splicing and transcription processes. Additionally,

Corresponding Author: Jiao Lv, BM; email: shhailj@163.com
Yunxing Shi, BM; email: shiyunxingshi@sina.com

circRNA can bind to RNA-binding protein (RBP) or interact with other RNAs through base-pair pairing[5]. CircRNA is conserved and differentially expressed in different species. Compared with linear RNA, circRNA is resistant to RNase and exerts strong stability. In recent years, circRNA has been well concerned as a promising diagnostic and therapeutic target for malignant tumors[6].

CircRNA has been reported to exert a great influence on the occurrence and development of GC. For example, circular RNA-ZFR regulates the expression of phosphate and tension homology deleted on chromosome ten (PTEN) by sponging miR-130a/miR-107. This can eventually inhibit the proliferative ability and promote the apoptosis of GC cells[7]. Cyclic RNA_LARP4 down-regulates LATS1 by sponging miR-424-5p, further inhibiting proliferative and invasive abilities of GC cells[8]. CircRNA_100269 is down-regulated in GC and inhibits cell growth by targeting miR-630[9]. Meanwhile, circ-CCDC66 is up-regulated in several types of tumors. Current studies[10,11] have also demonstrated that overexpression of circ-CCDC66 accelerates the malignant phenotypes of tumor cells and is closely regulated to poor prognosis. In this work, we explored the function of circ-CCDC66 in the progression of GC and the possible underlying mechanism.

Patients and Methods

Sample Collection

50 paired GC tissues and adjacent normal tissues were surgically resected from GC patients. Collected tissue samples were immediately preserved in liquid nitrogen for use. None of the enrolled GC patients received preoperative therapy, and they denied any family history. Informed consent was obtained from patients and their families before the study. This study was approved by the Ethics Committee of Hongkou Branch of Changhai Hospital.

Cell Culture and Transfection

GC cell lines (BGC-823, MGC-803, SGC-7901 and AGS) and gastric mucosal cell line (GES1) were provided by Cell Bank, Chinese Academy of Science (Shanghai, China). All cells were cultured in Roswell Park Memorial Institute-1640 medium (RPMI-1640; Gibco, Grand Island, NY, USA) containing 10% fetal bovine serum (FBS; Gibco, Grand Island, NY, USA), 100 U/mL penicillin and 0.1 mg/mL streptomycin in a 5% CO_2 and 37 °C incubator.

Until 70% of confluence, the cells were transfected with relative plasmid according to the instructions of Lipofectamine 2000 (Invitrogen, Carlsbad, CA, USA). After 6 hours, the fresh medium was replaced, followed by incubation for another 24 h.

RNA Extraction

Tissues were first fully lysed in 1 mL of TRIzol (Invitrogen, Carlsbad, CA, USA). After incubation at room temperature for 5 min, 200 μL of chloroform was added, mixed and stand at room temperature for 5 min. After centrifugation at 4 °C and 12,000 rpm for 15 min, the supernatant was transferred into a new RNase-free centrifuge tube. Isopropanol with the same volume of the supernatant was added for harvesting RNA precipitate by centrifugation. Extracted RNA was air dried, quantified and dissolved in diethyl pyrocarbonate (DEPC) water (Beyotime, Shanghai, China). RNA samples were preserved at -80°C for subsequent experiments.

Quantitative Real Time-Polymerase Chain Reaction (qRT-PCR)

Total RNA was extracted from tissues and cells using the TRIzol kit (Invitrogen, Carlsbad, CA, USA). The RNA concentration was measured by an ultraviolet spectrophotometer (Hitachi, Tokyo, Japan). Subsequently, extracted RNA was reverse transcribed into complementary deoxyribose nucleic acid (cDNA) according to the instructions of PrimeScriptTM RT MasterMix kit (Invitrogen, Carlsbad, CA, USA). Quantitative Real Time-Polymerase Chain Reaction (qRT-PCR) reaction conditions were as follows: 95°C for 2 min, followed by 40 cycles at 95°C for 1 min, 60°C for 1 min and 72°C for 1 min, and extension at 72°C for 7 min. The relative expression level of the target gene was calculated by the $2^{-\Delta\Delta Ct}$ method. Primer sequences used in this study were listed in Table I.

5-Ethynyl-2'- Deoxyuridine (EdU) Assay

Cells were first labeled with 50 μmol/L EdU (Solarbio, Beijing, China) at 37°C for 2 h. Subsequently, the cells were fixed with 4% paraformaldehyde for 30 min and incubated with Phosphate-Buffered Saline (PBS; Gibco, Grand Island, NY, USA) containing 0.5% Triton-100 for 20 min. After washing with PBS containing 3% bovine serum albumin (BSA), 100 μL of dying solution was added to each well, followed by 30-min incubation in the dark. After that, the nuclei were stained with 4',6-diamidino-2-phenylindole

Table I. The sequences related to the study.

Gene	Primer sequence
miR-1238-3p F:	GTCGTATCCAGTGCAGGG
miR-1238-3p R:	CGACGCTTCCTCGTCTG
Circ-CCDC66 F:	TCTCTTGGACCCAGCTCAG
Circ-CCDC66 R:	TGAATCAAAGTGCATTGCCC
GAPDH F:	AGCCACATCGCTCAGACAC
GAPDH R:	GCCCAATACGACCAAATCC
U6 F:	CTCGCTTCGGCAGCAGCACATATA
U6 R:	AAATATGGAACGCTTCACGA
LHX2 F:	CCGCCGCGATGCTGTTCCACAGTC
LHX2 R:	GAGTCATTAGAAAAGGTTGGTAAGAGTC

(DAPI; Sigma-Aldrich, St. Louis, MO, USA) for 5 min. Apollo-positive cells and DAPI-positive cells were captured using a confocal laser scanning microscope. Finally, the ratio of EdU-positive cells was calculated.

Colony Formation Assay

Cells were first seeded into 6-well plates with 300 cells per well and cultured for 10-14 days. Subsequently, the cells were fixed with 4% paraformaldehyde for 15 min and stained with 0.1% violet crystal for 30 min. After removing the staining solution, formed colonies were aired dried and observed under a microscope (Leica, Wetzlar, Germany). Finally, the number of colonies was counted.

Flow Cytometry Analysis

Transfected cells were incubated with 5 μL of Annexin V-FITC (fluorescein isothiocyanate) and 10 μL of Propidium Iodide (PI) in the dark for 15 min in strict accordance with Annexin V-FITC/PI apoptotic determination kit (Vazyme, Nanjing, China). Cell apoptosis was determined using BD FACSCanto II flow cytometry (BD Biosciences, Franklin Lakes, NJ, USA) and analyzed by FlowJo software.

Transwell Invasion Assay

The concentration of transfected cells was first adjusted to 3.0×10^5/mL. 100 μL/well suspension was added to the upper side of the transwell chamber (Millipore, Billerica, MA, USA) pre-coated with Matrigel (BD Biosciences, Franklin Lakes, NJ, USA). Meanwhile, 600 μL of medium containing 20% FBS was added to the lower side. After 48 h of incubation, invasive cells were fixed with methanol for 10-15 min, and dyed with 0.5% crystal violet for 20 min. The number of penetrating cells was counted under a microscope. 5 fields were randomly selected for each sample.

Dual-Luciferase Reporter Gene Assay

Wild-type and mutant-type Luciferase vectors of circ-CCDC66/LHX2 (LIM-homeobox domain 2) were first constructed, namely circ-CCDC66/LHX2 WT and circ-CCDC66/LHX2 MUT, respectively. Subsequently, the cells were co-transfected with circ-CCDC66/LHX2 WT or circ-CCDC66/LHX2 MUT and miRNA-1238-3p mimics or NC for 24 h. After that, the cells were fully lysed and centrifuged at 10,000 g for 5 min. Finally, 100 μL of supernatant was harvested for determining the Luciferase activity (Promega, Madison, WI, USA).

Western Blot

Total protein was extracted from cells using radioimmunoprecipitation assay (RIPA; Beyotime, Shanghai, China). The concentration of extracted protein was determined by the bicinchoninic acid (BCA) method. The protein samples were electrophoresed on polyacrylamide gels and transferred onto polyvinylidene difluoride (PVDF) membranes (Millipore, Billerica, MA, USA). After blocking with 5% skimmed milk, the membranes were incubated with primary antibodies (Cell Signaling Technology, Danvers, MA, USA) at 4°C overnight. After rinsing with Tris-Buffered Saline with Tween 20 (TBST; Sigma-Aldrich, St. Louis, MO, USA), the membranes were incubated with corresponding secondary antibody. Immunoreactive bands were exposed by enhanced chemiluminescence (ECL; Thermo Fisher Scientific, Waltham, MA, USA) and analyzed by Image Software (NIH, Bethesda, MD, USA).

Statistical Analysis

Statistical Product and Service Solutions (SPSS) 20.0 software was used for all statistical analyses. GraphPad Prism 7 (La Jolla, CA, USA) was used for figure editing. Experimental data

were expressed as mean ± standard deviation. Intergroup differences were analyzed by *t*-test. $p<0.05$ was considered statistically significant.

Results

Circ-CCDC66 Was Upregulated in GC Tissues and Cell Lines

The relative expression level of circ-CCDC66 in 50 paired GC tissues and adjacent normal tissues was determined by qRT-PCR. The results revealed that circ-CCDC66 was significantly up-regulated in GC tissues relative to adjacent normal tissues (Figure 1A). Identically, the circ-CCDC66 level was markedly higher in GC cell lines when compared with gastric mucosal cell line (Figure 1B). Therefore, we speculated that circ-CCDC66 might play a carcinogenic role in the progression of GC. By analyzing follow-up data, Kaplan-Meier curves indicated the significant worse prognosis of GC patients with a higher level of circ-CCDC66 (Figure 1C). Hence, the up-regulation of circ-CCDC66 predicted poor prognosis of GC patients.

Knockdown of Circ-CCDC66 Suppressed Proliferative and Invasive Abilities of GC Cells

Transfection efficacy of circ-CCDC66-siRNA in BGC-823 and MGC-803 cells was verified by qRT-PCR (Figure 2A). EdU assay illustrated that transfection of circ-CCDC66-siRNA in GC cells significantly decreased the ratio of EdU-positive cells (Figure 2B). Similarly, knockdown of circ-CCDC66 markedly reduced the number of formed colonies in GC cells (Figure 2C). Transwell assay showed that the number of invasive cells was remarkably reduced after transfection of circ-CCDC66-siRNA, suggesting inhibited invasive ability (Figure 2D). Knockdown of circ-CCDC66 significantly attenuated the proliferative and invasive abilities of GC cells.

Knockdown of Circ-CCDC66 Arrested Cell Cycle and Induced Apoptosis of GC

Flow cytometry revealed that GC cells were mainly arrested in the G0/G1 phase after transfection of circ-CCDC66-siRNA (Figure 3A). Meanwhile, the apoptotic rate of GC cells with circ-CCDC66 knockdown increased markedly (Figure 3B). The results demonstrated that up-regulation of circ-CCDC66 accelerated GC progression *via* accelerating cell cycle progression and suppressing cell apoptosis.

Circ-CCDC66 Could Bind to MiRNA-1238-3p

Potential miRNAs binding to circ-CCDC66 were predicted by bioinformatics method, and miRNA-1238-3p was screened out (Figure 4A). The binding relationship between circ-CCDC66 and miRNA-1238-3p was verified by the Dual-Luciferase reporter gene assay. The results showed that the Luciferase activity in BGC-823 cells co-transfected with miRNA-1238-3p mimics and circ-CCDC66 WT plasmid decreased significantly. However, no marked changes were observed in Luciferase activity after co-transfection with miRNA-1238-3p mimics and circ-CCDC66 MUT plasmid (Figure 4B). Furthermore, miRNA-1238-3p was identified significantly down-regulated in GC cell lines (Figure 4C). Transfection of circ-CCDC66-siRNA remarkably up-regulated miRNA-1238-3p expression in GC cells (Figure 4D). The above data demonstrated that circ-CCDC66

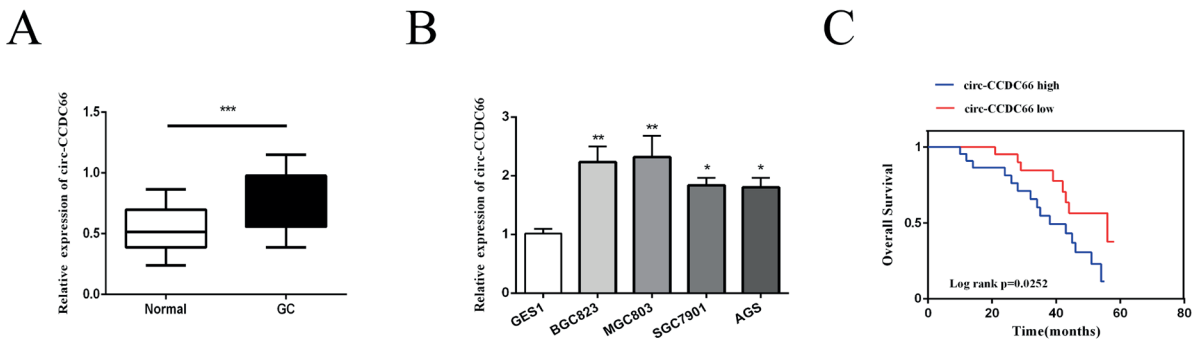

Figure 1. Circ-CCDC66 was up-regulated in GC tissues and cell lines. ***A,*** Relative level of circ-CCDC66 in 50 paired GC tissues and adjacent normal tissues determined by qRT-PCR. ***B,*** Relative level of circ-CCDC66 in GC cell lines (BGC-823, MGC-803, SGC-7901 and AGS) and gastric mucosal cell line GES1 determined by qRT-PCR. ***C,*** Kaplan-Meier curves revealed overall survival in GC patients with high or low level of circ-CCDC66. *$p<0.05$; **$p<0.01$; ***$p<0.001$.

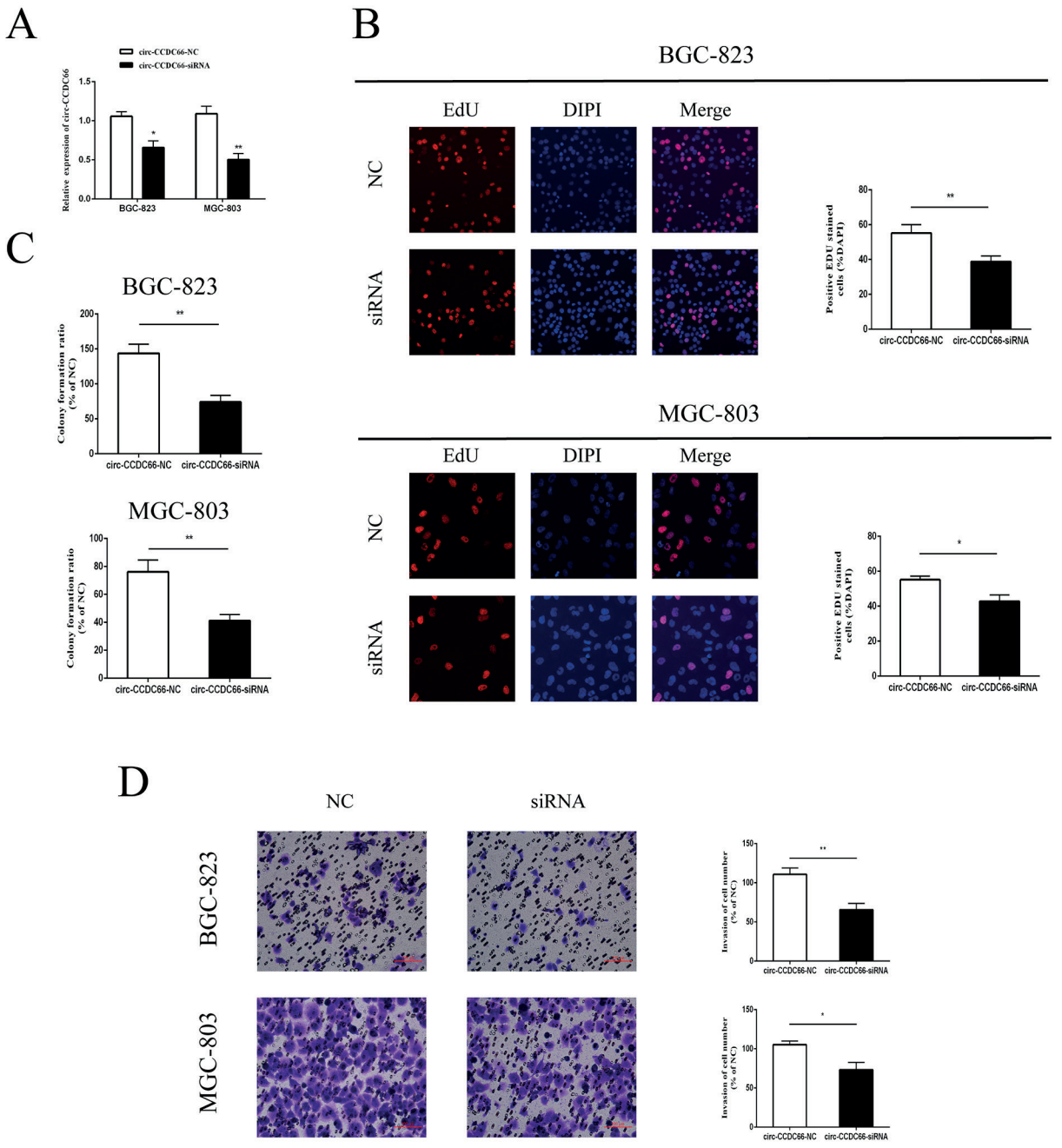

Figure 2. Knockdown of circ-CCDC66 suppressed proliferative and invasive abilities of GC cells. ***A,*** Transfection efficacy of circ-CCDC66-siRNA and circ-CCDC66-NC in BGC-823 and MGC-803 cells. ***B,*** EdU assay revealed the percentage of EdU-positive cells in BGC-823 and MGC-803 cells transfected with circ-CCDC66-siRNA or circ-CCDC66-NC (magnification 20×). ***C,*** Colony formation assay revealed the number of formed colonies in BGC-823 and MGC-803 cells transfected with circ-CCDC66-siRNA or circ-CCDC66-NC. ***D,*** Transwell assay revealed the number of migratory cells in BGC-823 and MGC-803 cells transfected with circ-CCDC66-siRNA or circ-CCDC66-NC (Magnification 20×). *p<0.05; **p<0.01.

could bind to miRNA-1238-3p and negatively regulate its expression in GC.

MiRNA-1238-3p Could Bind to LHX2

LXH2 was predicted as the target gene of miRNA-1238-3p that could directly bind to it (Figure 4E). Luciferase activity decreased remarkably in MGC-803 cells co-transfected with miRNA-1238-3p mimics and LXH2 WT plasmid, suggesting their binding relationship (Figure 4F). Subsequent qRT-PCR data showed that LHX2 was highly expressed in GC cells (Figure 4G).

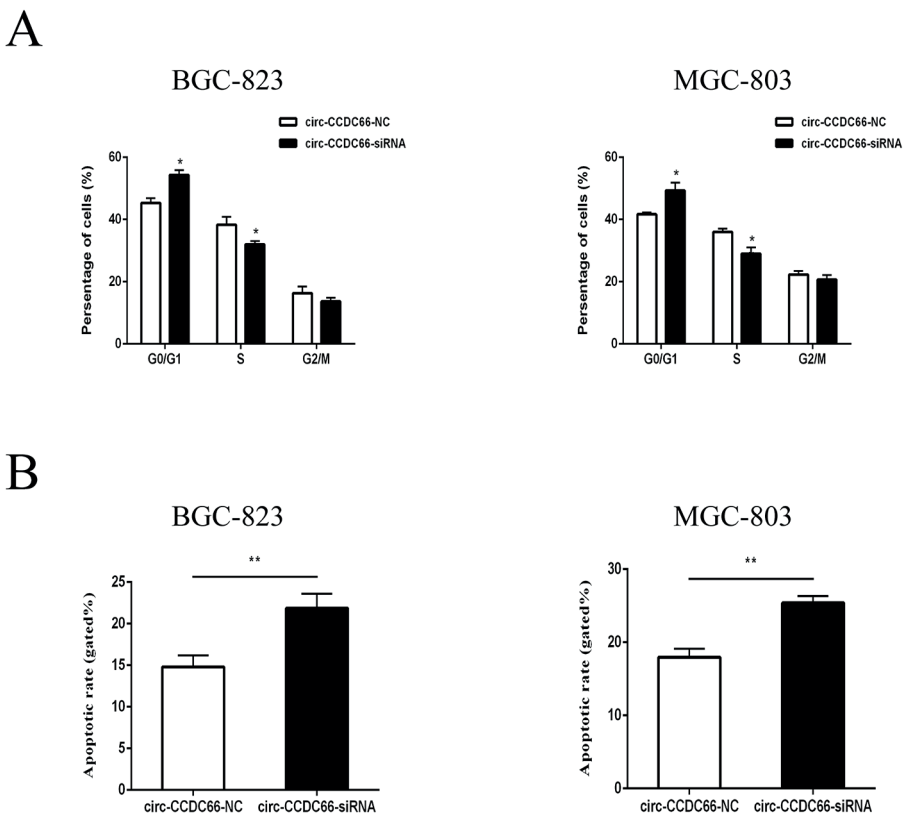

Figure 3. Knockdown of circ-CCDC66 arrested cell cycle and induced apoptosis of GC. ***A,*** Flow cytometry revealed the percentage of cells in G0/G1, S and G2/M phases in BGC-823 and MGC-803 cells transfected with circ-CCDC66-siRNA or circ-CCDC66-NC. ***B,*** Apoptotic rate in BGC-823 and MGC-803 cells transfected with circ-CCDC66-siRNA or circ-CCDC66-NC. **p*<0.05; ***p*<0.01.

Moreover, overexpression of miRNA-1238-3p markedly down-regulated both mRNA and protein levels of LHX2 (Figure 4H, 4I). Therefore, miRNA-1238-3p was proved to exert its biological role in GC progression *via* degrading LHX2.

Discussion

World Health Organization (WHO) reported that there are 1 million new cases of GC in 2018 globally, with more than 780,000 deaths. According to the reports proposed by the American Cancer Society, the 5-year survival of early-stage (Stage IA) and advanced-stage (Stage IV) GC patients is 71% and 4%, respectively. There are five layers of the stomach wall, and early-stage GC barely metastasizes. Local resection of GC in Stage I can effectively control the progression of GC[12]. Invasion and metastasis are important biological characteristics of malignant tumors, as well as the leading causes of tumor death[13]. Current studies have found that invasive and metastatic GC generally leads to malignant progression and poor prognosis. Therefore, genetic testing and screening as early as possible are vital methods for preventing tumor diseases[14]. Furthermore, it is of clinical importance to search for the molecular mechanism of GC invasion and metastasis.

CircRNA is abundantly present in plants and animals. It mainly existed in the cytoplasm of eukaryotic cells in the form of exon cyclization. Only a small part of circRNA presents in the nucleus in the form of intron cyclization[15]. CircRNA is structurally and functionally stable. The half-life of circRNA transcript is over 48 h, which is much longer than most of the mRNAs. The strong stability of circRNA allows it to become an important regulator in disease progression[16]. Previous studies have found that circRNA serves as an oncogene or tumor suppressor gene in malignancies. For instance, circVAPA is up-regulated in colorectal cancer and exerts a carcinogenic role by binding to miR-101[17]. CircBACH2 mediates

the progression of papillary thyroid carcinoma by sponging miR-139-5p to regulate LMO4 expression[18]. In addition, circRNA cTFRC acts as a sponge for microRNA-107 to promote bladder cancer progression[19].

In this study, we mainly explored the effects of circ-CCDC66 on the biological behaviors of GC cells, as well as the underlying mechanism. Our results found that circ-CCDC66 was remarkably up-regulated in GC tissues and cell lines. The results suggested that circ-CCDC66 might promote the progression of GC. Meanwhile, significantly worse overall survival was observed in GC patients with a higher level of circ-CCDC66.

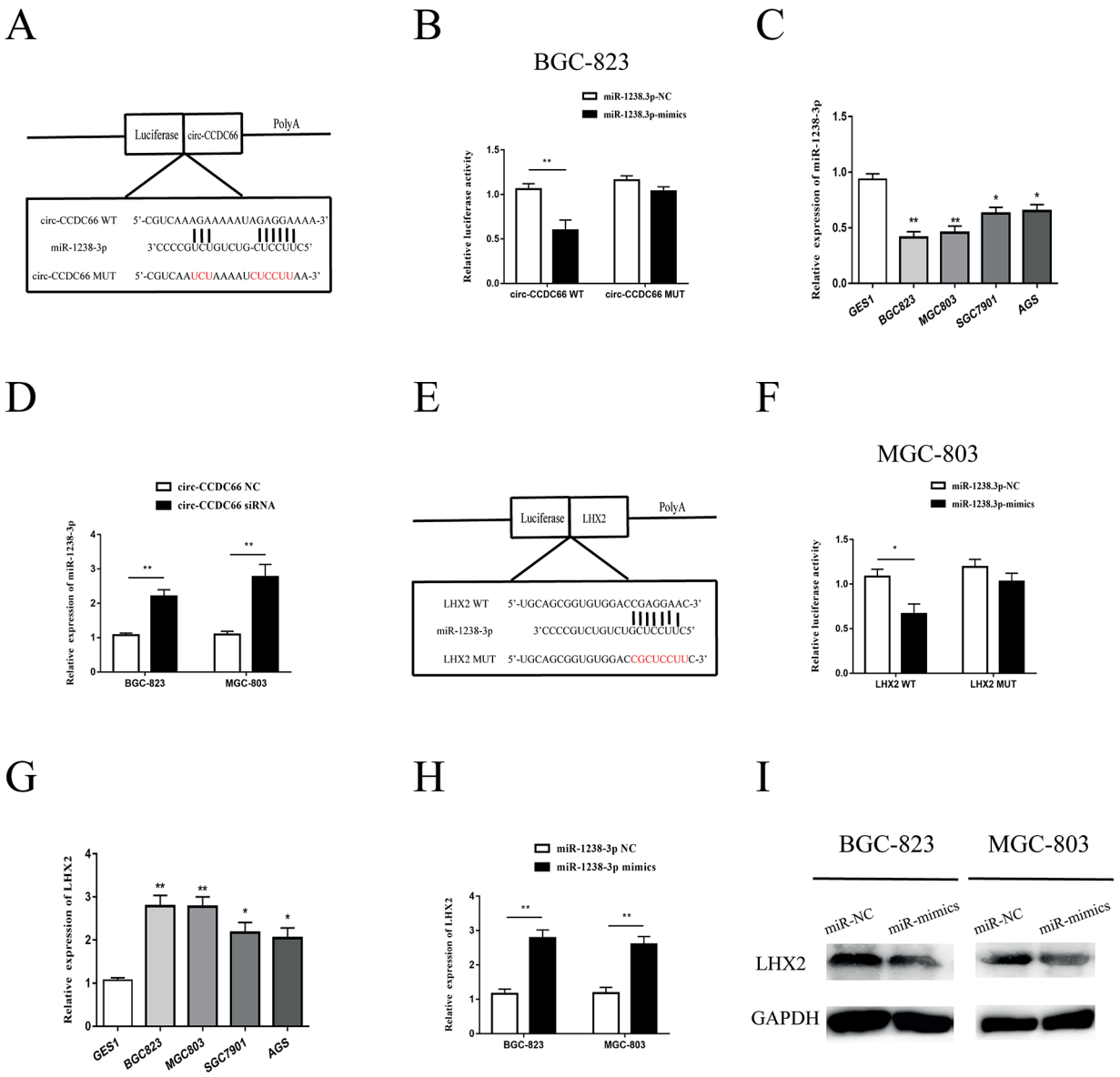

Figure 4. Circ-CCDC66 competed with LHX2 for binding to miR-1238-3p. ***A,*** Predicted binding sequences between circ-CCDC66 and miR-1238-3p. ***B,*** Luciferase activity in BGC-823 cells co-transfected with miR-1238-3p mimics/NC and circ-CCDC66 WT/MUT. ***C,*** Relative level of miR-1238-3p in GC cell lines (BGC-823, MGC-803, SGC-7901 and AGS) and gastric mucosal cell line GES1 determined by qRT-PCR. ***D,*** Relative level of miR-1238-3p in BGC-823 and MGC-803 cells transfected with circ-CCDC66-siRNA or circ-CCDC66-NC. ***E,*** Predicted binding sequences between LHX2 and miR-1238-3p. ***F,*** Luciferase activity in MGC-803 cells co-transfected with miR-1238-3p mimics/NC and LHX2 WT/MUT. ***G,*** Relative level of LHX2 in GC cell lines (BGC-823, MGC-803, SGC-7901 and AGS) and gastric mucosal cell line GES1 determined by qRT-PCR. ***H,*** Relative level of LHX2 in BGC-823 and MGC-803 cells transfected with miR-1238-3p mimics or NC. ***I,*** Protein level of LHX2 in BGC-823 and MGC-803 cells transfected with miR-1238-3p mimics or NC. *$p<0.05$; **$p<0.01$.

Knockdown of circ-CCDC66 markedly attenuated the proliferation and invasion of GC cells. Moreover, knockdown of circ-CCDC66 arrested cell cycle progression in G0/G1 phase and induced apoptosis of GC cells. In addition, through bioinformatics prediction and functional confirmation, we found that circ-CCDC66 could bind to miRNA-1238-3p and inhibit its expression.

Bioinformatics method predicted that circ-CCDC66 could bind to miRNA-1238-3p by competing with LHX2. As a member of the LIM homology domain protein family, LHX2 (LIM-homeobox domain 2) regulates lymphoid and neuronal differentiation, and brain and eye development[20,21]. LHX2 is also involved in the formation and development of a variety of tumor cells. For example, microRNA-506 inhibits the inactivation of the Wnt/β-catenin pathway by down-regulating LHX2, thereby inhibiting the growth and metastasis of nasopharyngeal carcinoma[22]. MiR-124 inhibits the migration and invasion of non-small cell lung cancer cells by down-regulating LHX2[23]. In the present study, miRNA-1238-3p expression was significantly down-regulated in GC cell lines, while LHX2 was up-regulated. Overexpression of miRNA-1238-3p in GC cells markedly decreased LHX2 expression. The above results suggested that circ-CCDC66 might up-regulate the expression of LHX2 by binding to miRNA-1238-3p, thus accelerating the progression of GC by promoting cell proliferation and invasion.

Conclusions

We found that circ-CCDC66 is up-regulated in both GC tissues and cell lines. Knockdown of circ-CCDC66 attenuates the proliferative and invasive abilities of GC cells. Furthermore, circ-CCDC66/miRNA-1238-3p/LHX2 axis may serve as a potential therapeutic target for GC.

Conflict of interest

The authors declare no conflicts of interest.

References

1) Wang J, Liu X. Correlation analysis between Helicobacter pylori infection status and tumor clinical pathology as well as prognosis of gastric cancer patients. Iran J Public Health 2018; 47: 1529-1536.
2) Luo W, Fedda F, Lynch P, Tan D. CDH1 gene and hereditary diffuse gastric cancer syndrome: molecular and histological alterations and implications for diagnosis and treatment. Front Pharmacol 2018; 9: 1421.
3) Griniatsos J, Trafalis D. Differences in gastric cancer surgery outcome between East and West: differences in surgery or different diseases? J BUON 2018; 23: 1210-1215.
4) Zhou LH, Yang YC, Zhang RY, Wang P, Pang MH, Liang LQ. CircRNA_0023642 promotes migration and invasion of gastric cancer cells by regulating EMT. Eur Rev Med Pharmacol Sci 2018; 22: 2297-2303.
5) Li WH, Song YC, Zhang H, Zhou ZJ, Xie X, Zeng QN, Guo K, Wang T, Xia P, Chang DM. Decreased expression of Hsa_circ_00001649 in gastric cancer and its clinical significance. Dis Markers 2017; 2017: 4587698.
6) Cheng J, Zhuo H, Xu M, Wang L, Xu H, Peng J, Hou J, Lin L, Cai J. Regulatory network of circRNA-miRNA-mRNA contributes to the histological classification and disease progression in gastric cancer. J Transl Med 2018; 16: 216.
7) Liu T, Liu S, Xu Y, Shu R, Wang F, Chen C, Zeng Y, Luo H. Circular RNA-ZFR inhibited cell proliferation and promoted apoptosis in gastric cancer by sponging miR-130a/miR-107 and modulating PTEN. Cancer Res Treat 2018; 50: 1396-1417.
8) Zhang J, Liu H, Hou L, Wang G, Zhang R, Huang Y, Chen X, Zhu J. Circular RNA_LARP4 inhibits cell proliferation and invasion of gastric cancer by sponging miR-424-5p and regulating LATS1 expression. Mol Cancer 2017; 16: 151.
9) Zhang Y, Liu H, Li W, Yu J, Li J, Shen Z, Ye G, Qi X, Li G. CircRNA_100269 is downregulated in gastric cancer and suppresses tumor cell growth by targeting miR-630. Aging (Albany NY) 2017; 9: 1585-1594.
10) Hsiao KY, Lin YC, Gupta SK, Chang N, Yen L, Sun HS, Tsai SJ. Noncoding effects of circular RNA CCDC66 promote colon cancer growth and metastasis. Cancer Res 2017; 77: 2339-2350.
11) Joseph NA, Chiou SH, Lung Z, Yang CL, Lin TY, Chang HW, Sun HS, Gupta SK, Yen L, Wang SD, Chow KC. The role of HGF-MET pathway and CCDC66 circRNA expression in EGFR resistance and epithelial-to-mesenchymal transition of lung adenocarcinoma cells. J Hematol Oncol 2018; 11: 74.
12) Du Y, Wei Y. Therapeutic potential of natural killer cells in gastric cancer. Front Immunol 2018; 9: 3095.
13) Xu J, Zhu J, Wei Q. Adjuvant radiochemotherapy versus chemotherapy alone for gastric cancer: implications for target definition. J Cancer 2019; 10: 458-466.
14) Matsuoka T, Yashiro M. Biomarkers of gastric cancer: current topics and future perspective. World J Gastroenterol 2018; 24: 2818-2832.
15) Fan L, Cao Q, Liu J, Zhang J, Li B. Circular RNA profiling and its potential for esophageal squamous cell cancer diagnosis and prognosis. Mol Cancer 2019; 18: 16.

16) Sun H, Tang W, Rong D, Jin H, Fu K, Zhang W, Liu Z, Cao H, Cao X. Hsa_circ_0000520, a potential new circular RNA biomarker, is involved in gastric carcinoma. Cancer Biomark 2018; 21: 299-306.

17) Li XN, Wang ZJ, Ye CX, Zhao BC, Huang XX, Yang L. Circular RNA circVAPA is up-regulated and exerts oncogenic properties by sponging miR-101 in colorectal cancer. Biomed Pharmacother 2019; 112: 108611.

18) Cai X, Zhao Z, Dong J, Lv Q, Yun B, Liu J, Shen Y, Kang J, Li J. Circular RNA circBACH2 plays a role in papillary thyroid carcinoma by sponging miR-139-5p and regulating LMO4 expression. Cell Death Dis 2019; 10: 184.

19) Su H, Tao T, Yang Z, Kang X, Zhang X, Kang D, Wu S, Li C. Circular RNA cTFRC acts as the sponge of MicroRNA-107 to promote bladder carcinoma progression. Mol Cancer 2019; 18: 27.

20) Miyoshi M, Kakinuma S, Kamiya A, Tsunoda T, Tsuchiya J, Sato A, Kaneko S, Nitta S, Kawai-Kitahata F, Murakawa M, Itsui Y, Nakagawa M, Azuma S, Nakauchi H, Asahina Y, Watanabe M. LIM homeobox 2 promotes interaction between human iPS-derived hepatic progenitors and iPS-derived hepatic stellate-like cells. Sci Rep 2019; 9: 2072.

21) Zhao Y, Mailloux CM, Hermesz E, Palkovits M, Westphal H. A role of the LIM-homeobox gene Lhx2 in the regulation of pituitary development. Dev Biol 2010; 337: 313-323.

22) Liang TS, Zheng YJ, Wang J, Zhao JY, Yang DK, Liu ZS. MicroRNA-506 inhibits tumor growth and metastasis in nasopharyngeal carcinoma through the inactivation of the Wnt/beta-catenin signaling pathway by down-regulating LHX2. J Exp Clin Cancer Res 2019; 38: 97.

23) Yang Q, Wan L, Xiao C, Hu H, Wang L, Zhao J, Lei Z, Zhang HT. Inhibition of LHX2 by miR-124 suppresses cellular migration and invasion in non-small cell lung cancer. Oncol Lett 2017; 14: 3429-3436.